BIOCHEMISTRY
including biophysical chemistry & molecular biology

Article

pubs.acs.org/biochemistry

Kinetic and Chemical Mechanism of Malate Synthase from *Mycobacterium tuberculosis*

Christine E. Quartararo and John S. Blanchard*

Department of Biochemistry, Albert Einstein College of Medicine, 1300 Morris Park Avenue, Bronx, New York 10461, United States

Supporting Information

ABSTRACT: Malate synthase catalyzes the Claisen-like condensation of acetyl-coenzyme A (AcCoA) and glyoxylate in the glyoxylate shunt of the citric acid cycle. The *Mycobacterium tuberculosis* malate synthase G gene, *glcB*, was cloned, and the N-terminal His_6-tagged 80 kDa protein was expressed in soluble form and purified by metal affinity chromatography. A chromogenic 4,4′-dithiodipyridine assay did not yield linear kinetics, but the generation of an active site-directed mutant, C619S, gave an active enzyme and linear kinetics. The resulting mutant exhibited kinetics comparable to those of the wild type and was used for the full kinetic analysis. Initial velocity studies were intersecting, suggesting a sequential mechanism, which was confirmed by product and dead-end inhibition. The inhibition studies delineated the ordered binding of glyoxylate followed by AcCoA and the ordered release of CoA followed by malate. The pH dependencies of k_{cat} and k_{cat}/K_{gly} are both bell-shaped, and catalysis depends on a general base (pK = 5.3) and a general acid (pK = 9.2). Primary kinetic isotope effects determined using [C^2H_3-*methyl*]acetyl-CoA suggested that proton removal and carbon−carbon bond formation were partially rate-limiting. Solvent kinetic isotope effects on k_{cat} suggested the hydrolysis of the malyl-CoA intermediate was also partially rate-limiting. Multiple kinetic isotope effects, utilizing D_2O and [C^2H_3-*methyl*]acetyl-CoA, confirmed a stepwise mechanism in which the step exhibiting primary kinetic isotope effects precedes the step exhibiting the solvent isotope effects. We combined the kinetic data and the pH dependence of the kinetic parameters with existing structural and mutagenesis data to propose a chemical mechanism for malate synthase from *M. tuberculosis*.

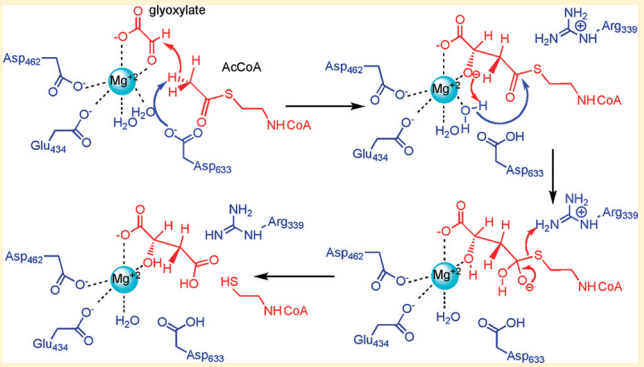

Malate synthase (MS) is an enzyme in the glyoxylate shunt of the citric acid cycle in a wide range of pro- and eukaryotes. The glyoxylate shunt has been implicated in the pathogenesis of several bacteria and fungi,[1] is not present in placental mammals,[2] and therefore represents an attractive drug target. The anaplerotic shunt allows for the assimilation of acetyl-coenzyme A (AcCoA) from fatty acid oxidation or de novo synthesis. Because the two decarboxylative steps of the TCA cycle are bypassed, respiration can continue when only two carbon substrates such as acetate and ethanol are available. The first reaction of the glyoxylate shunt occurs by the action of isocitrate lyase to convert isocitrate to succinate and glyoxylate. Malate synthase then catalyzes the Claisen-like condensation of glyoxylate and AcCoA to malate and coenzyme A (CoA).

The mechanism by which *Mycobacterium tuberculosis* (Mtb) enters into a nonreplicating, persistent state has been probed by the in vitro Wayne model.[3] In the Wayne model, Mtb bacilli gradually consume the available oxygen and survive in a non-replicating persistence state under these low-oxygen conditions. The hypoxic environment is thought to be similar to that inside the granulomatous lesions in which Mtb resides during latency. Under these conditions, there is an increase in the production of isocitrate lyase and glycine dehydrogenase, which generates glycine from glyoxylate.[4] Disruption of the isocitrate lyase gene has shown the necessity of the glyoxylate shunt in the survival of persistent Mtb,[5] establishing the physiological significance of this shunt in the persistence of Mtb. Mtb is a global health epidemic in which there were 9.4 million new cases in 2009.[6] Of these new infections, 60−90% will develop latent infection,[7] which cannot yet be targeted by any therapy. Furthermore, multiple and extensively drug resistant stains (MDR and XDR, respectively) have emerged, creating a dire need for novel drug targets.

Claisen condensation enzymes catalyze biosynthetic carbon−carbon bond formation typically in the elongation reactions of fatty acid or polyketide synthesis.[8] However, MS operates in the TCA cycle, catalyzing a Claisen-like condensation outside of these realms. Similar enzymes, which catalyze Claisen-like condensations outside of fatty acid and polyketide synthesis, have been kinetically characterized and are available for comparison: citrate synthase (CS) also in the TCA cycle, α-isopropylmalate synthase (α-IPMS) in leucine biosynthesis, and homocitrate synthase (HCS) in lysine biosynthesis. Each of these enzymes uses an AcCoA-derived carbon nucleophile and

Received: May 10, 2011
Revised: June 10, 2011
Published: July 5, 2011

an α-carbonyl-containing carboxylic acid substrate to create a CoA intermediate that is hydrolyzed to release product and CoA.[9−11] MS, α-IPMS, and HCS are all dependent on a divalent metal,[10,12,13] while CS utilizes two active site histidine residues.[14]

In this paper, we report the use of a characterized malate synthase mutant amenable to a continuous, chromogenic 4,4′-dithiodipyridine (DTP) assay. Initial velocity studies, dead-end and product inhibition, determined the steady-state ordered bi-bi kinetic mechanism for substrate binding and product release. The pH dependencies of the kinetic parameters, primary kinetic isotope effects, and solvent kinetic isotope effects were determined. Previously, the structure of malate synthase from Mtb was determined in complex with the metal cofactor Mg^{2+}, and both substrate glyoxylate [Protein Data Bank (PDB) entry 1N8I] and products CoA and malate (PDB entry 1N8W).[13] The primary sequence, predetermined structural data, and newly presented kinetic data provide the basis for a proposed chemical mechanism.

MATERIALS AND METHODS

Materials. All chemicals were purchased from Sigma Aldrich. The pET-28a(+) vector was from Novagen. Cloning enzymes and T7 express competent *Escherichia coli* cells were from New England Biolabs, and primers were from Invitrogen. DNase and Complete EDTA-free protease were from Roche; 99.9% deuterated water was from Cambridge Isotope Laboratories.

Cloning, Overexpression, and Purification of MS. The Mtb *glcB* gene (Rv1837c) was PCR amplified from H37Rv DNA using the forward primer 5′-ATCCCGCTCATATGACAGATCGCGTGTCGGTG-3′ and reverse primer 5′-ATCCCGCTCTCGAGCTAGCGGGCCGCATCGTCACC-3′. Restriction sites for NdeI and XhoI, respectively, are underlined. The PCR fragment was cloned into a pET-28a(+) vector containing an N-terminal His_6 tag. After the sequence had been verified, the recombinant plasmid was transformed into T7 express competent cells. Six liters of LB containing 30 μg/mL kanamycin were inoculated with a 3 mL overnight starter culture and incubated at 37 °C. At an A_{600} of ∼0.6−0.8, cells were induced with 0.5 mM IPTG and incubated at 20 °C overnight. Cells were harvested by centrifugation, and the pellets were resuspended in 50 mM Tris (pH 8.0) containing 400 mM NaCl and 5% glycerol (buffer A), sonicated, and centrifuged at 17000 rpm for 35 min to remove cellular debris. Batch purification was performed with a Ni-NTA agarose column. The column was washed with buffer A, and the protein was eluted with 350 mM imidazole in buffer A. The His_6 tag was removed by thrombin cleavage in 50 mM Tris containing 50 mM NaCl, 5% glycerol, 400 units of thrombin, 1 mM DDT, and 1 mM $CaCl_2$. After cleavage, the protein was dialyzed and stored in 50 mM Tris (pH 7.0) containing 50 mM NaCl at −20 °C.

C619S MS Mutant. C619S MS was prepared using the QuikChange II Site-Directed Mutagenesis Kit and standard PCR modifications with forward primer 5′-GTTGATCAAGGTGTCGGCTCATCGAAGGTGCCCGACATC-3′ and reverse primer 5′-GATGTCGGGCACCTTCGATGAGCCGACACCTTGATCAAC-3′, where the mutated codons are underlined. Expression of the mutant plasmid followed the same protocol that was used for the wild type, except with induction by 1 mM IPTG. The mutant was purified as described above with the following modifications. Buffer A became 50 mM Tris (pH 8.0) containing 250 mM NaCl. One tablet of Complete EDTA-free protease inhibitor mix, 250 μg of DNAase, and 10 mM $MgCl_2$ were added to the pellets resuspended in 75 mL of buffer A before sonication. After similar batch purification, dialysis was performed to remove the His_6 tag in 20 mM Tris (pH 8.4) containing 150 mM NaCl, 5% glycerol, 400 units of thrombin, 1 mM DDT, and 1 mM $CaCl_2$. After dialysis, the protein was then applied to a Superdex200 HiLoad 26/60 size exclusion column using a buffer that consisted of 50 mM HEPES (pH 7.0) containing 150 mM NaCl and 5% glycerol at a flow rate of 1 mL/min. Malate synthase-containing fractions identified by SDS−PAGE were combined and judged to be ∼95% pure. Aliquots (15 μM) were stored in 50 mM HEPES (pH 7.0) containing 150 mM NaCl, 25 mM $MgCl_2$, and 55% glycerol at −20 °C.

Protein Concentration. The concentration of WT MS was determined using the Bio-Rad protein assay using bovine serum albumin as a standard. The concentration of C619S MS was determined using A_{280} and an extinction coefficient of 79000 M^{-1} cm^{-1}.[15,16]

Measurement of Enzymatic Activity. Enzymatic activity was determined by a coupled 4,4′-dithiodipyridine (DTP) assay at 324 nm. Reactions were conducted in 50 mM HEPES (pH 7.5) containing 15 mM $MgCl_2$ and 200 μM DTP, substrates AcCoA and glyoxylate, until a final volume of 1 mL was reached. All assays were performed at 25 °C, and 1.5 nM WT or C619S MS was added to initiate the reaction. Reactions were monitored spectrophotometrically until 10% substrate conversion to product. Rates were calculated using the molar extinction coefficient of DTP, 19800 M^{-1} cm^{-1}, and the total enzyme concentration (E_t).

Data Fitting. All data fitting was performed with GraphPad Prism version 5.0d. In all graphs, the points are the mean of experimental duplicates, and the error bars are the standard deviation. The solid lines are the result of fitting to the denoted equation.

Initial Velocity of WT and C619S MS. Initial kinetic parameters were estimated by saturating with one substrate and varying the concentration of the other substrate. The resulting curve was fit to eq 1

$$v = (VS)/(K_m + S) \quad (1)$$

where V is the maximal velocity and S is the concentration of the varied substrate. Initial velocity studies were conducted at fixed, saturating concentrations of glyoxylate and varying concentrations of AcCoA and vice versa. The resulting patterns were fit globally to eq 2 for a sequential kinetic mechanism

$$v = (VAB)/(K_{ia}K_b + K_aB + K_bA + AB) \quad (2)$$

where V is the maximal velocity, A and B are the substrate concentrations, K_a and K_b are the respective Michaelis constants for each substrate, and K_{ia} is the inhibition constant for substrate A.

pH Dependence of C619S MS Activity. The pH dependencies of the kinetic parameters were determined in 50 mM buffer at the desired pH [sodium acetate (pH 4.5−5.0), MES (pH 5.0−6.5), HEPES (pH 6.5−8.0), and TAPS (pH 8.0−10.0)] under saturating conditions of AcCoA and varying concentrations of glyoxylate. The resulting k_{cat} and k_{cat}/K_{gly} data were fit to eq 3, which describes a bell-shaped curve to

obtain both the pK_a, the negative log of the acid dissociation constant, and pK_b, the negative log of the base dissociation constant, where c is the pH-independent plateau value.

$$\log k_{cat} \text{ or } \log k_{cat}/K_{gly} = \log[- c/(1 + K_b/10^{-pH} + 10^{-pH}/K_a)] \quad (3)$$

Dead-End and Product Inhibition. The dead-end inhibitor, dethio-CoA, was synthesized as previously described.[17] It was purified on a Synergi Fusion-RP column (250 mm × 10.0 mm, Phenomenex) using a linear gradient of buffer A, 0.2% trifluoroacetic acid in water, and buffer B, 0.2% trifluoroacetic acid in acetonitrile. Fractions having an A_{260} that eluted with the same retention time were pooled and lyophilized overnight. Mass spectrometry was used to confirm the presence of dethio-CoA. The samples were stored in H_2O at −20 °C. Product inhibition by malate and dead-end inhibition by dethio-CoA were tested with variable amounts of inhibitor, and both varying concentrations of AcCoA and glyoxylate. Data were globally fit to eq 4 for competitive inhibition, eq 5 for uncompetitive inhibition, or eq 6 for noncompetitive inhibition

$$v = (VS)/[K_m(1 + I/K_{is}) + S] \quad (4)$$

$$v = (VS)/[K_m + S(1 + I/K_{ii})] \quad (5)$$

$$v = (VS)/[K_m(1 + I/K_{is}) + S(1 + I/K_{ii})] \quad (6)$$

where S is the varied substrate concentration, I is inhibitor concentration, K_{is} is the inhibition constant for the slope, K_{ii} is the inhibition constant for the intercept, and K_m is the Michaelis constant of substrate S.

Kinetic Isotope Effects. Synthesis of [C^2H_3-*methyl*]-AcCoA was conducted by acetylation of coenzyme A[18] with excess deuterated acetic anhydride [$(CD_3CO)_2O$]. The CoA was dissolved in D_2O and combined with 5 mL of anhydrous *N*,*N*-dimethylformamide and 10 μL of triethylamine (TEA). The mixture was stirred for 10 min at 25 °C. Deuterated acetic anhydride was added to 2 mL of DMF and the mixture added dropwise to the stirring mixture. The purification, mass spectrometric identification, and storage were identical to those for dethio-CoA. Assays were performed under saturating glyoxylate conditions and varying concentrations of AcCoA and [C^2H_3-*methyl*]AcCoA. The results were globally fit to eq 7

$$v = (VS)/[K(1 + F_iE_{V/K}) + S(1 + F_iE_V)] \quad (7)$$

where V is the maximal velocity, S is the concentration of AcCoA or [C^2H_3-*methyl*]AcCoA, F_i is the fraction of isotope (0 or 1), $E_{V/K}$ is the effect on $k_{cat}/K_m - 1$, and E_V is the effect on $k_{cat} - 1$. The pH dependence of the KIEs was measured at pH 5.5 and 6.5 (MES), pH 7.5 (HEPES), and pH 8.5 and 9.5 (TAPS).

Solvent Kinetic Isotope Effects. Solvent kinetic isotope effects were measured with saturating concentrations of glyoxylate and varying concentrations of AcCoA and globally fit to eq 7 where $F_i = 0$ for H_2O and $F_i = 0.93$ for D_2O. A viscosity control of 9% glycerol[19] did not show any effect on either V or V/K_{AcCoA}. A proton inventory was determined under saturating conditions of both AcCoA and glyoxylate at 10% increments from 0 to 90% D_2O.

Multiple Kinetic Isotope Effects. MKIEs were measured with saturating concentrations of glyoxylate and varying concentrations of [C^2H_3-*methyl*]AcCoA in H_2O and 93% D_2O, and varying concentrations of AcCoA and [C^2H_3-*methyl*]AcCoA in 93% D_2O. Data were globally fit to eq 7.

RESULTS AND DISCUSSION

Cloning, Expression, and Purification. For WT MS, PCR amplification of the *glcB* gene resulted in a single fragment, 2.2 kb, of the expected size, which sequencing confirmed lacked any mutation introduced by PCR. The C619S mutant form of MS was similarly sequenced to confirm only the designed mutation. Overexpression yielded soluble proteins of the expected mass, 80 kDa. Approximately 14 mg of pure WT MS and 22 mg of pure C619S MS were obtained per liter of culture. SDS−PAGE was used to determine the molecular mass and >90% purity.

Measurement of Enzyme Activity. WT MS failed to display linear kinetics above pH 7.0 using the DTP assay (Figure S1 of the Supporting Information). The activity of WT MS was confirmed by directly monitoring thioester cleavage of substrate AcCoA by the decrease in absorbance at 232 nm between pH 4.8 and 8.5 (data not shown). A close examination of the crystallographically determined structure of Mtb MS (PDB entry 1N8I)[13] showed Cys619 to be near the active site. Site-directed mutagenesis was used to produce C619S, which was active using a DTP assay and displayed linear kinetic traces from pH 4.5 to 10. A lag phase was observed, but the addition of 25 mM $MgCl_2$ to the storage buffer and 15 mM $MgCl_2$ to the reaction mixture caused the lag to disappear. The similarity of the kinetic constants obtained with the WT and C619S mutant suggested that the C619S mutant could be used to continue kinetic evaluation using the more sensitive and robust DTP assay. All data further reported are for C619S MS.

Kinetic Mechanism. Initial velocity studies were performed to distinguish between a sequential mechanism and a ping-pong mechanism. When the glyoxylate concentration was varied at fixed AcCoA concentrations and fit to a sequential mechanism (Figure 1A), the following parameters were determined: $k_{cat} = 23 \pm 3\ s^{-1}$, $K_{gly} = 30 \pm 6$ μM, $K_{AcCoA} = 10 \pm 3$ μM, and $K_{ia} = 3 \pm 2$ μM. When the AcCoA concentration was varied at fixed glyoxylate concentrations, a similar intersecting pattern was observed and the fit to a sequential mechanism (Figure 1B) yielded similar kinetic parameters. On the basis of the observed intersecting lines in both double-reciprocal plots (Figure 1A,B), a steady-state ordered mechanism is proposed.

Product and dead-end inhibition studies were performed to determine the order of substrate binding and product release. Product inhibition with malate was competitive against glyoxylate (Figure 1C) and noncompetitive against AcCoA (Figure 1D), suggesting that glyoxylate binds first and malate is released last, supporting an ordered kinetic mechanism. Dead-end inhibition by dethio-CoA was uncompetitive versus glyoxylate (Figure 1E) and competitive versus AcCoA (Figure 1F), suggesting that the dead-end inhibitor dethio-CoA binds to a different enzyme form than glyoxylate and to the same enzyme form as AcCoA. Together with the product inhibition results, the formation of an enzyme−glyoxylate complex is expected before the AcCoA can bind to create the ternary complex. The proposed kinetic mechanism is shown in Scheme 1 in which the ordered binding of glyoxylate is followed by AcCoA, CoA is released first, and malate is released last.

Studies in the yeast enzyme[20] proposed a sequential random kinetic mechanism, on the basis of the initial velocity double-reciprocal plots intersecting on the x-axis at $-1/K_m$, indicating

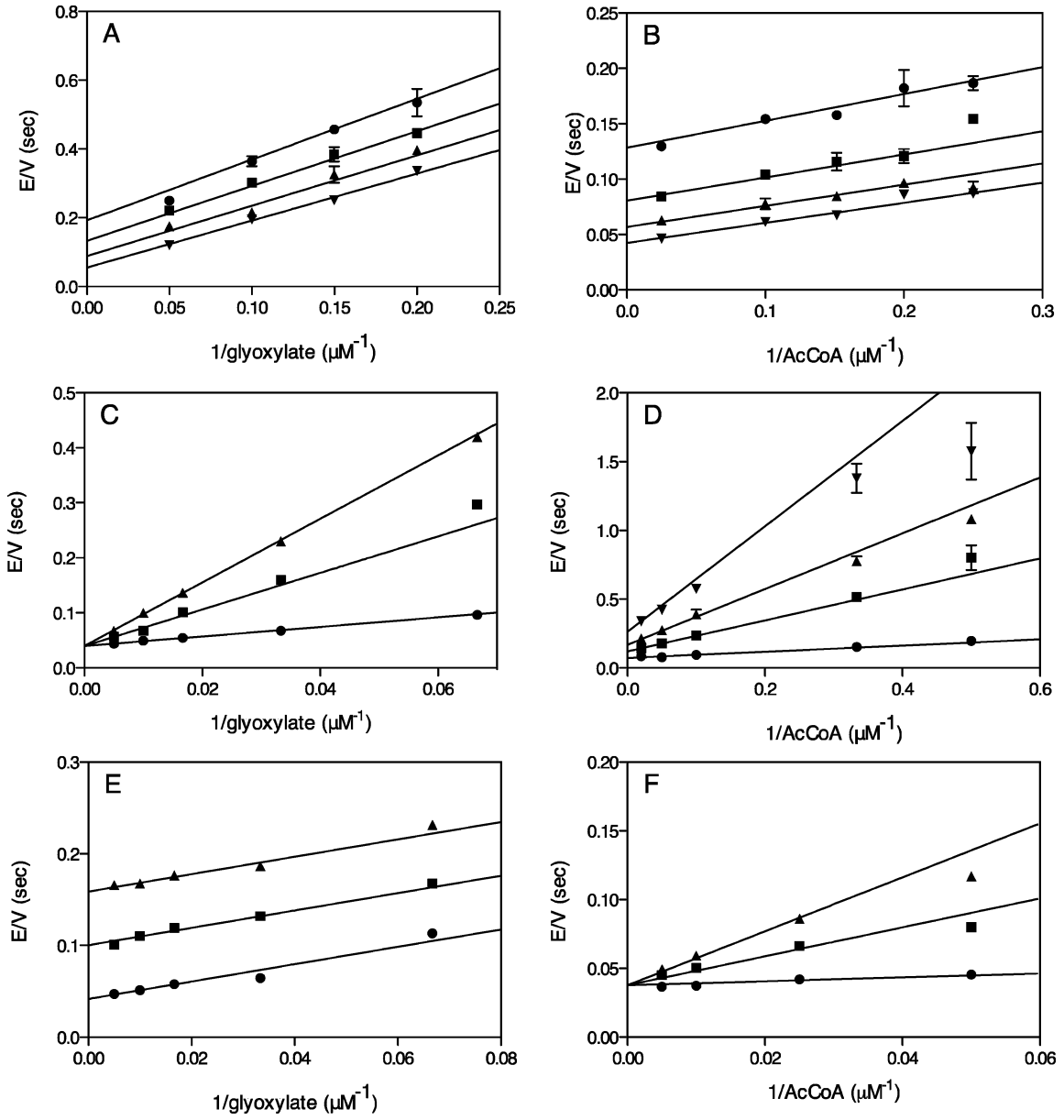

Figure 1. Elucidation of the kinetic mechanism of C619S MS. (A) Initial velocity at varying concentrations of glyoxylate (5−20 μM) and different fixed concentrations of AcCoA: 3 (●), 5 (■), 10 (▲), and 40 μM (▼). Equation 2 determined the following: k_{cat} = 23 ± 3 s^{-1}, K_{gly} = 30 ± 6 μM, K_{AcCoA} = 10 ± 3 μM, and K_{ia} = 3 ± 2 μM. (B) Initial velocity at varying concentrations of AcCoA (4−40 μM) and different fixed concentrations of glyoxylate: 10 (●), 20 (■), 40 (▲), and 100 μM (▼). Global fitting to eq 2 determined the following: k_{cat} = 30 ± 2 s^{-1}, K_{gly} = 29 ± 4 μM, K_{AcCoA} = 5 ± 1 μM, and K_{ia} = 0.7 ± 0.7 μM. (C) Product inhibition by malate with 25 μM AcCoA and 15−200 μM glyoxylate at different fixed concentrations of malate: 0 (●), 25 (■), and 50 mM (▲). Global fitting to eq 4 determined inhibition constant K_{is} = 9 ± 1 mM. (D) Product inhibition by malate with 30 μM glyoxylate and 2−50 μM AcCoA at different fixed concentrations of malate: 0 (●), 25 (■), 50 (▲), and 100 mM (▼). Global fitting of to eq 6 determined the following: K_{is} = 6 ± 1 mM, and K_{ii} = 38 ± 7 mM. (E) Dead-end inhibition by dethio-AcCoA with 25 μM AcCoA and 15−200 μM glyoxylate at different fixed concentrations of dethio-AcCoA: 0 (●), 25 (■), and 50 μM (▲). Global fitting to eq 5 determined inhibition constant K_{ii} = 18 ± 1 μM. (F) Dead-end inhibition with 300 μM glyoxylate and 20−200 μM AcCoA at different fixed concentrations of dethio-AcCoA: 0 (●), 25 (■), and 50 μM (▲). Global fitting to eq 4 determined K_{is} = 4 ± 1 μM.

that the binding of one substrate is not affected by the binding of the other substrate. This initial velocity pattern was not observed in Mtb MS, and the Mtb MS inhibition studies also support an ordered, not random, kinetic mechanism. Mtb α-isopropylmalate synthase displays an intersecting initial velocity pattern, proceeding by a random kinetic mechanism.[9] Homocitrate synthase and citrate synthase both exhibit ordered binding, with their respective non-AcCoA substrates, α-ketoglutarate and oxaloacetate, binding first.[10,11]

pH Dependence of C619S MS Activity. To probe the chemical mechanism of MS, the pH dependencies of k_{cat} and k_{cat}/K_{gly} (Figure 2) were examined between pH 4.5 and 10.0 to determine the protonation states of enzyme and substrates necessary for binding and catalysis. The pH−rate profile was determined using saturating conditions of AcCoA and varying concentrations of glyoxylate, but control points were added to confirm the same bell-shaped dependence of log k_{cat} when the AcCoA concentration was varied. These points were not

dx.doi.org/10.1021/bi2007299 | Biochemistry 2011, 50, 6879−6887

Scheme 1. Ordered Bi-Bi Kinetic Mechanism of Malate Synthase

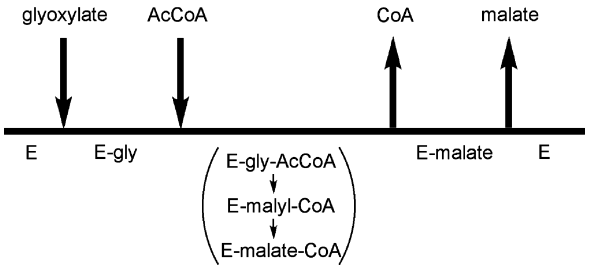

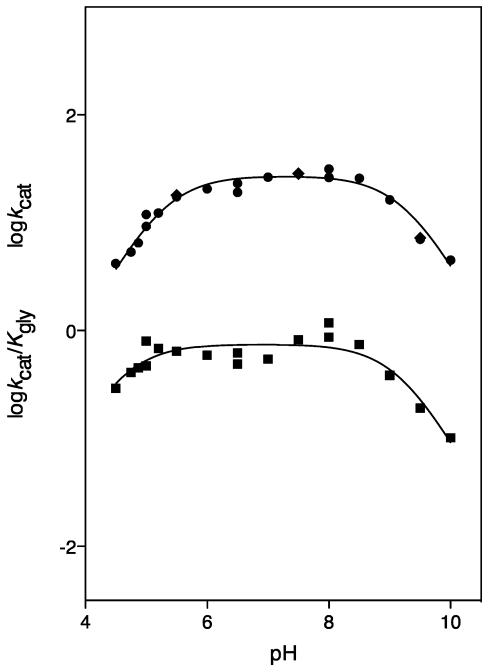

Figure 2. pH dependence of C619S MS. k_{cat} determined at saturating AcCoA and varying glyoxylate concentrations (●). Fitting to eq 3 determined pK_a = 5.3 ± 0.1 and pK_b = 9.2 ± 0.1. Superimposed (◆) are data for saturating glyoxylate and varied AcCoA concentrations from the control reactions in the pH dependence of the KIEs. k_{cat}/K_{gly} is represented by squares where global fitting to eq 3 gave a pK_a of 4.6 ± 0.2 and a pK_b of 9.1 ± 0.3.

included during fitting to eq 3. A bell-shaped curve was observed for log k_{cat}, with a group that must be deprotonated for catalysis exhibiting a pK_a value of 5.3 ± 0.1 and a group that must be protonated for catalysis exhibiting a pK_b value of 9.2 ± 0.1. The pH dependence of log k_{cat}/K_{gly} reports on ionizable groups responsible for binding and catalysis and was also bell-shaped (pK_a = 4.6 ± 0.2, and pK_b = 9.1 ± 0.3). A similar bell-shaped pH−rate profile was seen for log k_{cat} and log k_{cat}/K_m for both substrates of homocitrate synthase, evidence of acid−base catalysis.[21] On the basis of crystal structures of *M. tuberculosis*[13] and mutagenesis studies,[22] Asp633 is proposed to be the catalytic base corresponding to a pK_a of 5.3 ± 0.1 in log k_{cat} and Arg339 is proposed to be the catalytic acid corresponding to a pK_b of 9.2 ± 0.1 in log k_{cat}. The mutagenesis studies were conducted with the *E. coli* enzyme, but the primary sequences of the *E. coli* and Mtb malate synthases are 58% identical and 74% similar. Additionally, superimposition of crystal structures Mtb 1N8W[13] and *E. coli* 1D8C[23] revealed nearly identical active sites, and the superimposable location of Mtb MS residues Asp633 and Arg339 and the corresponding *E. coli* residues.

Kinetic Isotope Effects. Primary kinetic isotope effects were measured at pH 7.5, determining ^{D}V and $^{D}V/K_{AcCoA}$ with AcCoA and [C^2H_3-*methyl*]AcCoA (Figure 3A). Normal

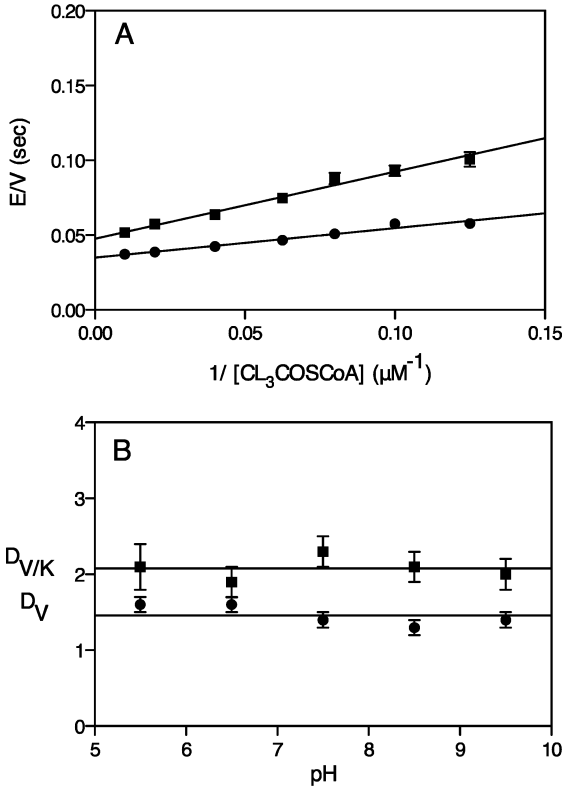

Figure 3. Kinetic isotope effects utilizing deuterated AcCoA. (A) KIEs at saturating glyoxylate (300 μM) and varying (8−100 μM) AcCoA concentrations, where L is H (●) or deuterated AcCoA (■) at pH 7.5; ^{D}V = 1.4 ± 0.1 and $^{D}V/K_{AcCoA}$ = 2.3 ± 0.3 where L is D. (B) ^{D}V and $^{D}V/K_{AcCoA}$ were determined with a method identical to that used for panel A at 1 pH unit increments from pH 5.5 to 9.5. The lack of pH dependence was fit with the lines ^{D}V = 1.46 and $^{D}V/K_{AcCoA}$ = 2.08, the average of the respective KIEs from each pH.

primary kinetic isotope effects were observed with a ^{D}V of 1.4 ± 0.1 and a $^{D}V/K_{AcCoA}$ of 2.3 ± 0.3, thus confirming that abstraction of proton from the AcCoA methyl group is at least partially rate-limiting. The unusual observation that $^{D}V/K_{AcCoA} > {}^{D}V$ suggests that AcCoA is not sticky and there is a step after proton abstraction that is also partly rate-limiting, lowering ^{D}V. However, because ^{D}V is not unity, it is unlikely that product release is substantially rate-limiting.

The primary KIEs from pH 5.5 to 9.5 were found to be independent of pH (Figure 3B), and therefore, the abstraction of a proton from the AcCoA methyl group is rate-limiting across all determined pH values. Primary KIEs using [C^2H_3-*methyl*]AcCoA have been previously reported for the yeast enzyme to exhibit normal isotope effects on both V and V/K (1.3 ± 0.1)[24] and an effect of 1.37 for both V and V/K.[20]

Solvent kinetic isotope effects were examined in 93% D_2O at pH 7.5, a region where the kinetic parameters are insensitive to small changes in pH (Figure 4A). There was no observed SKIE on $^{D_2O}V/K_{AcCoA}$, but a normal effect on ^{D_2O}V of 1.7 ± 0.1. This normal solvent kinetic isotope effect on V suggests that a step

dx.doi.org/10.1021/bi2007299 | *Biochemistry* 2011, 50, 6879−6887

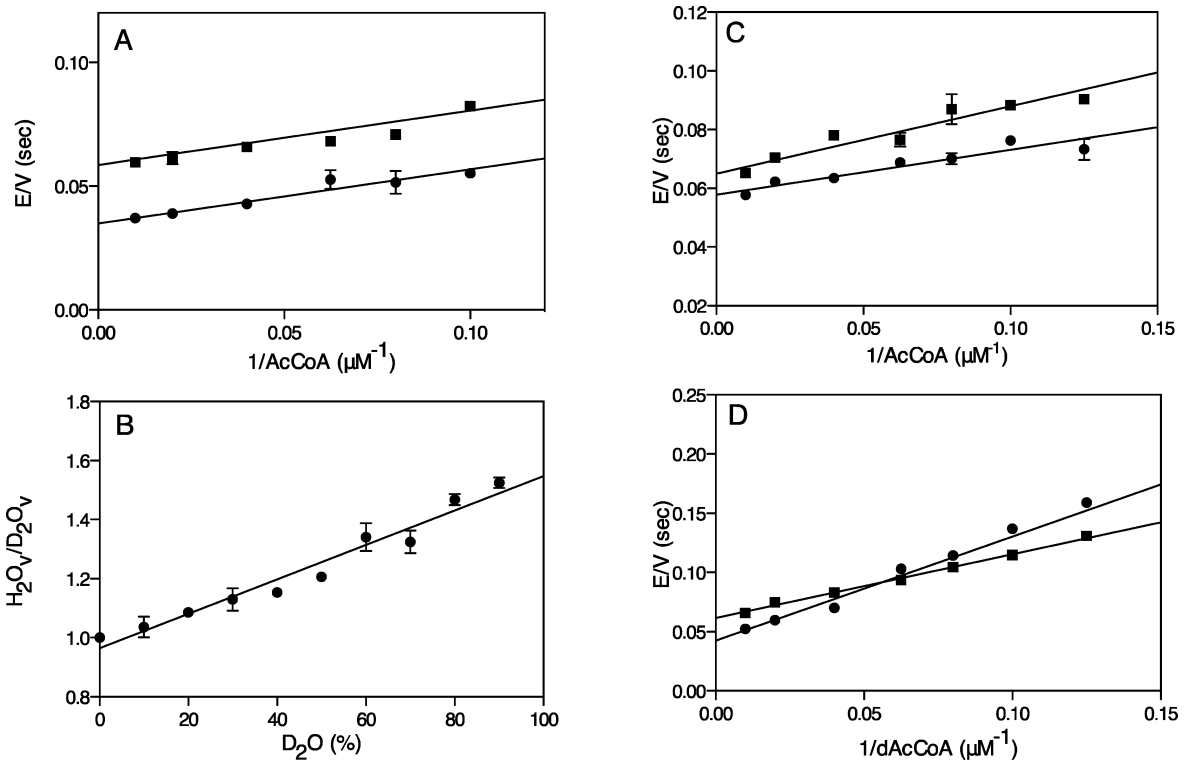

Figure 4. Solvent kinetic isotope effects in D_2O. (A) SKIEs at saturating glyoxylate (300 μM) and varying AcCoA (10−100 μM) concentrations at pH 7.5 in H_2O (●) or 93% D_2O (■) (^{D_2O}V = 1.7 ± 0.1, and $^{D_2O}V/K_{AcCoA}$ = 1.0 ± 0.3). (B) Proton inventory at saturating glyoxylate (300 μM) and saturating AcCoA (100 μM) concentrations at pH 7.5 in 10% D_2O increments from 0 to 90%. (C) Multiple kinetic isotope effects using saturating glyoxylate (300 μM) and varying deuterated AcCoA (8−100 μM) (■) or AcCoA (●) concentrations in D_2O ($^{D_2O}V_{[C^2H_3-methyl]AcCoA}$ = 1.1 ± 0.1, and $^{D_2O}V/K_{[C^2H_3-methyl]AcCoA}$ = 1.5 ± 0.3). (D) Multiple kinetic isotope effects using saturating glyoxylate (300 μM) and varying deuterated AcCoA (8−100 μM) concentrations in H_2O (●) and D_2O (■) ($^{D_2O}V_{[C^2H_3-methyl]AcCoA}$ = 1.5 ± 0.1, and $^{D_2O}V/K_{[C^2H_3-methyl]AcCoA}$ = 0.6 ± 0.1).

in catalysis is sensitive to solvent isotopic composition. We suggest that the ^{D_2O}V isotope effect reports on the abstraction of a proton from the metal-bound water that initiates the hydrolysis of the malyl-CoA intermediate. The lack of a solvent effect on V/K_{AcCoA} suggests the step that is sensitive to solvent isotopic composition is not the same step as the deprotonation of AcCoA responsible for the primary kinetic isotope effect. Further, it argues that upon attack of the resonance-stabilized AcCoA anion on metal-bound glyoxylate the resulting malyl-CoA exists as the alkoxide form. Finally, the unitary value of $^{D_2O}V/K_{AcCoA}$ also argues for the chemically reasonable order of carbon−carbon bond formation preceding hydrolysis.

In a proton inventory experiment (Figure 4B), $^{H_2O}V/^{D_2O}V$ was determined in 10% increments from 0 to 90% D_2O. A linear proton inventory is indicative of a single solvent-derived proton involved in the step that is solvent sensitive. While a linear fit is shown, the possibility of a slight curvilinear dependence, corresponding to more that one proton being "in flight", was recognized. In extrapolating the data to 100% D_2O, we obtained a value of 1.6, within error of the experimentally determined ^{D_2O}V of 1.7 ± 0.1.

Multiple kinetic isotope effects were determined in two ways. In the first, the primary kinetic isotope effect was determined in 93% D_2O. As seen in Figure 4C, the magnitudes of both $^{D}V/K_{AcCoA}$ and ^{D}V were reduced compared to their values in H_2O [$^{D}V/K_{AcCoA}$ = 1.5 ± 0.3 (D_2O) vs 2.3 ± 0.3 (H_2O), and ^{D}V = 1.1 ± 0.3 (D_2O) vs 1.4 ± 0.1 (H_2O)]. These data are most consistent with a stepwise mechanism[25] in which formation of the carbon−carbon bond and thioester hydrolysis occur in two separate steps. The sequential nature of the two chemical steps is also supported by the earlier findings where $^{D}V/K_{AcCoA} > {}^{D}V$. The use of the double-isotope fractionation test by Clark et al.[24] also supported the stepwise reaction of malate synthase using [C^2H_3-*methyl*]AcCoA and [^{13}C]-glyoxylate labeled at the aldehyde carbon.[24] In this analysis, the addition of [C^2H_3-*methyl*]AcCoA decreased the ^{13}C effect, indicating that [C^2H_3-*methyl*]AcCoA increased the energy barrier of the first step (abstraction of a proton from the methyl group of AcCoA) and thus decreased the KIE of the second step, formation of a bond with ^{13}C. Prior to these two steps, they proposed a third partially rate-limiting step that was unaffected by isotopic distribution in either substrate. The second MKIE was to determine the SKIE using [C^2H_3-*methyl*]AcCoA in H_2O and D_2O (Figure 4D). The MKIE on $^{D_2O}V_{[C^2H_3-methyl]AcCoA}$ of 1.5 ± 0.1 was normal, and the MKIE on $^{D_2O}V/K_{[C^2H_3-methyl]AcCoA}$ of 0.6 ± 0.1 was inverse. The most curious feature of this result was the appearance of a nonunitary, inverse $^{D_2O}V/K$ effect with deuterated AcCoA.

Inverse solvent kinetic isotope effects are commonly attributed to proton transfer processes to groups that exhibit inverse fractionation factors. Known causes of inverse fractionation factors include the increased viscosity of D_2O versus that of H_2O,[19] metal-bound waters (~0.7−1.0), and sulfhydryl groups (~0.5).[26] The possible contribution by viscosity is unlikely given the lack of an effect on V and V/K_{AcCoA} in 9% glycerol (data not shown). However, both metal-bound water and sulfhydryl

dx.doi.org/10.1021/bi2007299 | *Biochemistry* 2011, 50, 6879−6887

Scheme 2. Proposed Chemical Mechanism of Malate Synthase

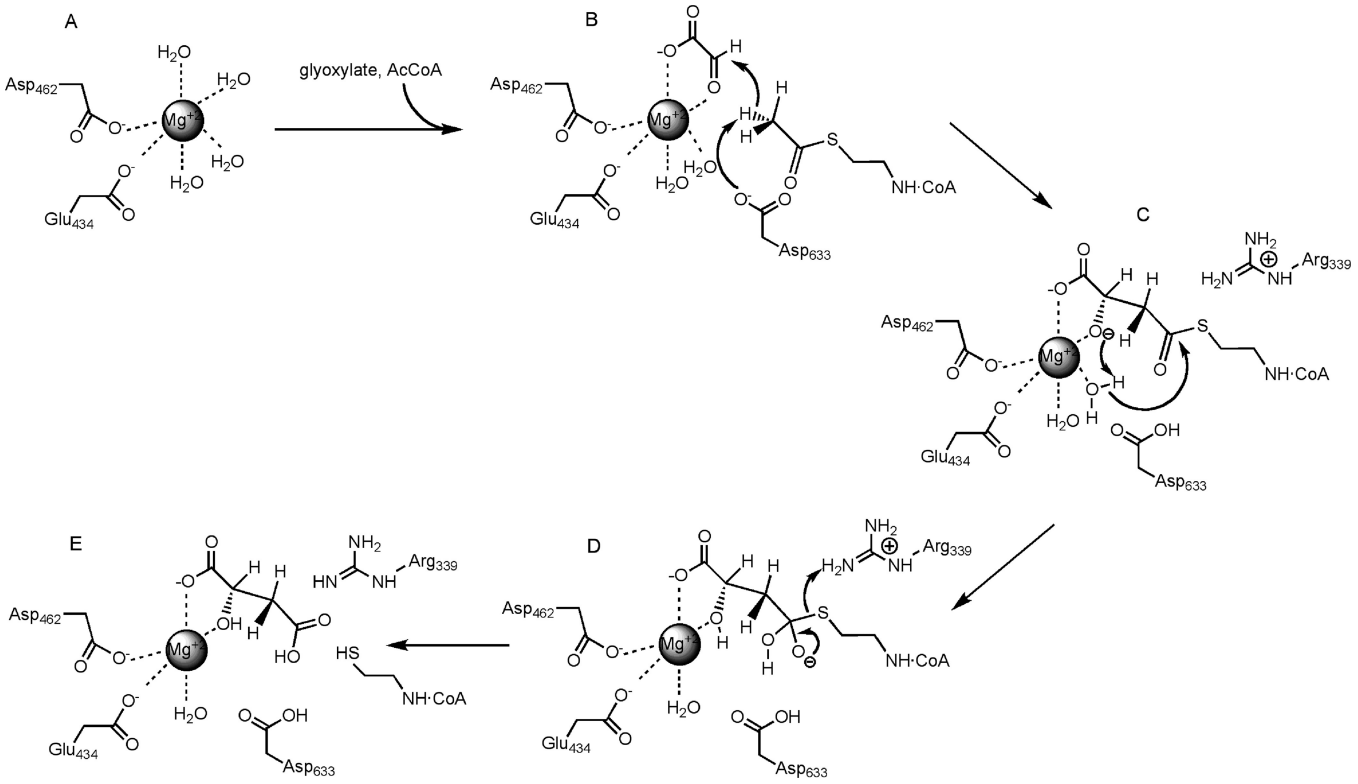

groups are potential sources of an inverse effect in the MS reaction. Because of the position of Mg^{2+} at the end of the tubelike active site, and coordination by glyoxylate and malate, it is clear the Mg^{2+} ion serves to bind and polarize substrates and is a central component of the reaction. Because water molecules additionally coordinate Mg^{2+}, it is a possibility that the metal-bound water is the source of the inverse MKIE. Because the inverse SKIE is observed on $^{D}V/K_{AcCoA}$, solvent isotopic composition is affecting a step preceding AcCoA deprotonation and C−C bond formation and possibly the precatalytic partially rate-limiting step identified by Clark et al.[24] on the basis of the smaller intermolecular isotope effect (1.37) compared to the intramolecular primary KIE of 3.7.[27] The data do not provide convincing evidence of the exact origin of the inverse MKIE. One possibility includes global solvent reorganization after the binding of substrates, allowing for a conformational change that would appropriately position the two reactants. Another alternative is that this isotope effect is due to the dehydration of the hydrated aldehyde form of glyoxylate to the aldehyde observed to coordinate Mg^{2+} and react with AcCoA.

Proposed Mechanism. The proposed mechanism starts (Scheme 2A) with the Mg^{2+} ion octahedrally coordinated by the carboxylate side chains of conserved residues Glu434 and Asp462, and four water molecules as seen in the crystal structure 1N8I[13] (Scheme 2B). As required by the inhibition studies, glyoxylate binds first, displacing two of the metal-coordinated water molecules. α-Isoketovalerate, the substrate of Mg^{2+}-dependent α-isopropylmalate synthase, and α-ketoglutarate, the substrate of Zn^{2+}-dependent homocitrate synthase, are also positioned for the reaction by coordination to the divalent metal ion.[9,21] In MS, in Scheme 2B after the binding of AcCoA, the conserved Asp633 is the catalytic base exhibiting a pK_a value of 4.6−5.3, which abstracts a proton from AcCoA. This step is partially rate-limiting as evidenced by the primary deuterium kinetic isotope effect on V. In support of this, the analogous *E. coli* residue, Asp631, was mutated to Asn and exhibited no activity.[22] The resulting nucleophile attacks glyoxylate to form the malyl-CoA intermediate, which we draw as the alkoxide (Scheme 2C). We propose the formation of the malyl-CoA intermediate is the first irreversible step (Scheme 2C). The alkoxide serves to remove the proton from an adjacent metal-bound water, creating the hydroxide anion that attacks the carbonyl of the thioester intermediate. This step is the origin of ^{D_2O}V, which requires a solvent-derived proton transfer step, and in a step separate from that of [C^2H_3-*methyl*]AcCoA (Scheme 2D). The tetrahedral intermediate now decomposes with the generation of the two products. We propose Arg339 acts as a catalytic acid to protonate the leaving group, the thiolate of CoA, and is the group observed in the k_{cat} profile with a pK_b value of 9.2 ± 0.1. In the Mtb MS-CoA-malate structure, one of the ureido nitrogens is 3.6 Å from the thiol of CoASH. The analogous *E. coli* residue, Arg338, was mutated to Lys and exhibited only 6.6% of the WT activity[22] (Scheme 2E). The ordered release of CoA followed by L-malate completes the catalytic cycle.

Conclusions. In this work, we examine Mtb malate synthase, from the currently untargeted glyoxylate shunt. We report a steady-state ordered bi-bi kinetic mechanism. Additionally, we propose a Mg^{2+}-centered reaction mechanism in which glyoxylate binds first to the enzyme, coordinating Mg^{2+}. Asp633 acts as a catalytic base to abstract a proton from AcCoA, generating a nucleophilic attack on glyoxylate to form a malyl-CoA intermediate. A water proton is abstracted by the intermediate alkoxide, which generates a hydroxyl nucleophile that attacks the malyl-CoA intermediate. Arg339 protonates the CoA, prompting the decomposition of the tetrahedral

dx.doi.org/10.1021/bi2007299 | *Biochemistry* 2011, 50, 6879–6887

intermediate, and the ordered release of the products CoA and malate completes the catalytic sequence. The new kinetic and chemical mechanistic data could support inhibitor design for malate synthase and thus target the glyoxylate shunt and persistence in Mtb.

■ ASSOCIATED CONTENT

Supporting Information

Time course comparison of WT MS and C619S MS activity (Figure S1). This material is available free of charge via the Internet at http://pubs.acs.org.

■ AUTHOR INFORMATION

Corresponding Author

*Department of Biochemistry, Albert Einstein College of Medicine, 1300 Morris Park Ave., Bronx, NY 10461. Phone: (718) 430-3096. Fax: (718) 430-8565. E-mail: blanchar@aecom.yu.edu.

Funding

This work was supported by the National Institutes of Health Grants AI33696 to J.S.B. and T32 AI007501 to C.E.Q.

■ ACKNOWLEDGMENTS

We thank Dr. Hua Xu for his assistance with the synthesis of dethio-CoA and [C^2H_3]AcCoA, Edward Nieves for performing mass spectrometry, Dr. Subray Hegde for his assistance in the cloning and purification of WT MS, and Clarissa Czekster and An Vandemeulebroucke for their insightful discussions.

■ ABBREVIATIONS

AcCoA, acetyl-coenzyme A; α-IPMS, α-isopropylmalate synthase; CoA, coenzyme A; CS, citrate synthase; DDT, dithiothreitol; DMF, *N*,*N*-dimethylformamide; DTP, 4,4′-dithiodipyridine; EDTA, ethylenediaminetetraacetic acid; E_t, total enzyme; gly, glyoxylate; HCS, homocitrate synthase; HEPES, *N*-(2-hydroxyethyl)piperazine-*N*′-2-ethanesulfonic acid; IPTG, isopropyl β-D-thiogalactopyranoside; KIE, kinetic isotope effect; LB, Luria broth; MES, 2-(*N*-morpholino)-ethanesulfonic acid; MS, malate synthase; Mtb, *M. tuberculosis*; MDR, multidrug resistant; MKIE, multiple kinetic isotope effect; Ni-NTA, nickel nitriloacetic acid; PCR, polymerase chain reaction; SDS−PAGE, sodium dodecyl sulfate−polyacrylamide gel electrophoresis; SKIE, solvent kinetic isotope effect; TAPS, *N*-[tris(hydroxymethyl)methyl]-3-aminopropanesulfonic acid; TCA, tricarboxylic acid; Tris, tris(hydroxymethyl)aminomethane; TEA, triethylamine; TFA, trifluoroacetic acid; WT, wild type; XDR, extensively drug resistant.

■ REFERENCES

(1) Dunn, M. F., Ramirez-Trujillo, J. A., and Hernandez-Lucas, I. (2009) Major roles of isocitrate lyase and malate synthase in bacterial and fungal pathogenesis. *Microbiology 155*, 3166−3175.

(2) Kondrashov, F. A., Koonin, E. V., Morgunov, I. G., Finogenova, T. V., and Kondrashova, M. N. (2006) Evolution of glyoxylate cycle enzymes in Metazoa: Evidence of multiple horizontal transfer events and pseudogene formation. *Biol. Direct 1*, 31.

(3) Wayne, L. G., and Sohaskey, C. D. (2001) Nonreplicating persistence of *Mycobacterium tuberculosis*. *Annu. Rev. Microbiol. 55*, 139−163.

(4) Wayne, L. G., and Lin, K. Y. (1982) Glyoxylate metabolism and adaptation of *Mycobacterium tuberculosis* to survival under anaerobic conditions. *Infect. Immun. 37*, 1042−1049.

(5) McKinney, J. D., Honer zu Bentrup, K., Munoz-Elias, E. J., Miczak, A., Chen, B., Chan, W. T., Swenson, D., Sacchettini, J. C., Jacobs, W. R. Jr., and Russell, D. G. (2000) Persistence of *Mycobacterium tuberculosis* in macrophages and mice requires the glyoxylate shunt enzyme isocitrate lyase. *Nature 406*, 735−738.

(6) World Health Organization (2011) 2010/2011 Tuberculosis Global Facts. http://www.who.int/tb/publications/2010/factsheet_tb_2010.pdf (March 11, 2011).

(7) Manabe, Y. C., and Bishai, W. R. (2000) Latent *Mycobacterium tuberculosis*: Persistence, patience, and winning by waiting. *Nat. Med. 6*, 1327−1329.

(8) Heath, R. J., and Rock, C. O. (2002) The Claisen condensation in biology. *Nat. Prod. Rep. 19*, 581−596.

(9) de Carvalho, L. P., and Blanchard, J. S. (2006) Kinetic and chemical mechanism of α-isopropylmalate synthase from *Mycobacterium tuberculosis*. *Biochemistry 45*, 8988−8999.

(10) Andi, B., West, A. H., and Cook, P. F. (2004) Kinetic mechanism of histidine-tagged homocitrate synthase from *Saccharomyces cerevisiae*. *Biochemistry 43*, 11790−11795.

(11) Kurz, L. C., Drysdale, G., Riley, M., Tomar, M. A., Chen, J., Russell, R. J., and Danson, M. J. (2000) Kinetics and mechanism of the citrate synthase from the thermophilic archaeon *Thermoplasma acidophilum*. *Biochemistry 39*, 2283−2296.

(12) de Carvalho, L. P., and Blanchard, J. S. (2006) Kinetic analysis of the effects of monovalent cations and divalent metals on the activity of *Mycobacterium tuberculosis* α-isopropylmalate synthase. *Arch. Biochem. Biophys. 451*, 141−148.

(13) Smith, C. V., Huang, C. C., Miczak, A., Russell, D. G., Sacchettini, J. C., and Honer zu Bentrup, K. (2003) Biochemical and structural studies of malate synthase from *Mycobacterium tuberculosis*. *J. Biol. Chem. 278*, 1735−1743.

(14) Remington, S. J. (1992) Structure and mechanism of citrate synthase. *Curr. Top. Cell. Regul. 33*, 209−229.

(15) ProtParam Tool (2010) http://ca.expasy.org/tools/protparam.html (August 19, 2010).

(16) Pace, C. N., Vajdos, F., Fee, L., Grimsley, G., and Gray, T. (1995) How to measure and predict the molar absorption coefficient of a protein. *Protein Sci. 4*, 2411−2423.

(17) Chase, J. F., Middleton, B., and Tubbs, P. K. (1966) A coenzyme A analogue, desulpho-coA; preparation and effects on various enzymes. *Biochem. Biophys. Res. Commun. 23*, 208−213.

(18) Wilson, I.B. (1952) Preparation of acetyl coenzyme A1. *J. Am. Chem. Soc. 74*, 3205−3206.

(19) Karsten, W. E., Lai, C. J., and Cook, P. F. (1995) Inverse Solvent Isotope Effects in the NAD-Malic Enzyme Reaction Are the Result of the Viscosity Difference between D_2O and H_2O: Implications for Solvent Isotope Effect Studies. *J. Am. Chem. Soc. 117*, 5914−5918.

(20) Durchschlag, H., Biedermann, G., and Eggerer, H. (1981) Large-scale purification and some properties of malate synthase from baker's yeast. *Eur. J. Biochem. 114*, 255−262.

(21) Qian, J., West, A. H., and Cook, P. F. (2006) Acid-base chemical mechanism of homocitrate synthase from *Saccharomyces cerevisiae*. *Biochemistry 45*, 12136−12143.

(22) Anstrom, D. M., Kallio, K., and Remington, S. J. (2003) Structure of the *Escherichia coli* malate synthase G:pyruvate:acetyl-coenzyme A abortive ternary complex at 1.95 Å resolution. *Protein Sci. 12*, 1822−1832.

(23) Howard, B.R., Endrizzi, J. A., and Remington, S. J. (2000) Crystal structure of *Escherichia coli* malate synthase G complexed with magnesium and glyoxylate at 2.0 Å resolution: Mechanistic implications. *Biochemistry 39*, 3156−3168.

(24) Clark, J. D., O'Keefe, S. J., and Knowles, J. R. (1988) Malate synthase: Proof of a stepwise Claisen condensation using the double-isotope fractionation test. *Biochemistry 27*, 5961−5971.

(25) Hermes, J.D., Roeske, C. A., O'Leary, M. H., and Cleland, W. W. (1982) Use of multiple isotope effects to determine enzyme mechanisms and intrinsic isotope effects. Malic enzyme and glucose-6-phosphate dehydrogenase. *Biochemistry 21*, 5106−5114.

(26) Quinn, D. M., and Sutton, L. D. (1991) Theoretical Basis and Mechanistic Utility of Solvent Isotope Effects. In *Enzyme Mechanism from Isotope Effects* (Cook, P. F., Ed.) pp 115−116, CRC Press, Boca Raton, FL.

(27) Lenz, H., and Eggerer, H. (1976) Enzymic generation of chiral acetates. A quantitative evaluation of their configurational assay. *Eur. J. Biochem. 65*, 237−246.